Ecological Indicators 146 (2023) 109775

Contents lists available at ScienceDirect

Ecological Indicators

journal homepage: www.elsevier.com/locate/ecolind

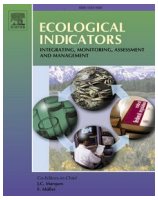

Intra-annual sediment dynamic assessment in the Wei River Basin, China, using the AIC functional-structural connectivity index

Zhenni Wu [a,*], Jantiene E.M. Baartman [a], João Pedro Nunes [a,b], Manuel López-Vicente [c]

[a] Soil Physics and Land Management Group, Wageningen University, Wageningen, the Netherlands
[b] CE3C – Centre for Ecology, Evolution, and Environmental Changes, Faculdade de Ciências, Universidade de Lisboa, 1749-016 Lisboa, Portugal
[c] AQUATERRA Research Group, Advanced Scientific Research Centre, University of A Coruña, CICA-UDC. As Carballeiras s/n, Campus de Elviña, La Coruña 15071, Spain

ARTICLE INFO

Keywords:
Sediment connectivity
Aggregated index of connectivity
Structural and functional
Soil erosion
Loess Plateau

ABSTRACT

Hydrological and sediment dynamics have changed considerably on the Chinese Loess Plateau during the last six decades due to large scale land use changes and numerous water regulation actions. Understanding the mechanism of sediment transport change and its effects is of great importance to food and environmental security. Numerical approaches are useful to map and assess spatio-temporal patterns in sediment dynamics. This study evaluates monthly and annual sediment connectivity in the Wei River Basin (134,800 km^2) at the basin and sub-basin scales using the aggregated index of sediment connectivity (AIC). For the first time, this index is applied on this relatively large regional scale. The two objectives were to (1) evaluate the performance of the AIC at the regional scale, addressing substantial differences among areas, and (2) analyze how each AIC sub-factor co-determines the monthly sediment and connectivity patterns. Results show that AIC has strong or moderate positive correlation with sediment yield from 15 out of 23 stations in the Wei and Jing sub-basin. The Jing sub-basin has the highest sediment connectivity due to degraded vegetation, while the Beiluo sub-basin has the lowest sediment connectivity on average due to better ecological restoration. Within the year, sediment connectivity is highest in April and lowest in January, due to the rainfall regime and intra-annual land cover variations. Among the AIC factors, the rainfall factor has the highest effect on sediment connectivity, implying that functional connectivity (graded by rainfall and soil cover) determines sediment dynamics more than structural connectivity (mainly determined by topography and soil permeability). This study provides one of the first large-scale estimates of spatial and temporal sediment connectivity from hillslopes to river stream and including large reservoirs, which can be further employed to implement regional ecological construction works and environmental catchment management.

1. Introduction

Soil erosion remains an environmental issue globally that affects human life in many aspects. It threatens agriculture and food safety by removing fertile soil, soil moisture, nutrients and microorganisms in the surface soil during soil loss (Pimentel, 2006). In addition, off-site effects including sedimentation and siltation can lead to water pollution (Issaka and Ashraf, 2017) and increased flood risk and shortening reservoir lifespan (López-Vicente et al., 2011). The Chinese Loess Plateau is one of the most eroded regions in the world. Even though soil erosion rates in the entire area have drastically decreased in last two decades (Fu et al., 2011; Wen and Zhen, 2020; Wen et al., 2020), it can reach 15,000 t km^{-2} yr^{-1} and an area of almost 100,000 km^2 is estimated to have soil erosion rates higher than 8,000 t km^{-2} yr^{-1} (NDRC et al. 2010). Thus, a lot of attention has been and still is paid to erosion and sediment yield in the Loess Plateau (Gu et al., 2019; Tong et al., 2020; Huo et al., 2021).

Sediment connectivity is a promising concept in erosion research, addressing the sediment transfer from sources to sinks within a system (Wohl et al., 2019; Hooke and Souza 2021), and the response of the system to both external and internal forces, such as climate change and anthropogenic structures (Lisenby et al., 2019). Connectivity can be divided into two categories: structural connectivity and functional connectivity (Turnbull et al. 2008; López-Vicente et al., 2016; Cossart and Fressard 2017). Structural connectivity represents the physical

* Corresponding author.
E-mail address: zhenni.wu@wur.nl (Z. Wu).

https://doi.org/10.1016/j.ecolind.2022.109775
Received 3 October 2022; Received in revised form 29 November 2022; Accepted 4 December 2022

linkages of the system at a certain point in time – usually using long term annual mean values, while functional connectivity relates to dynamic processes – the transfer of water and sediment through the system over a specific period in time (Heckmann et al., 2018). Connectivity is often estimated by using modelling approaches, such as graph theory-based network analysis and connectivity indices (Hooke and Souza, 2021). Indices can present one or a few proxy variables such as topographic characteristics, network structure, and vegetation characteristics that would affect connectivity (Bracken et al., 2015). An elaborated review of connectivity indices was done by Heckmann et al. (2018). In 2008, a raster-based connectivity index named Index of Connectivity (IC) was proposed by Borselli et al. (2008), which was used successfully to qualitatively address potential sediment connectivity between catchment components. Due to the simple and clear calculation scheme, the IC has been widely applied in different regions (López-Vicente et al., 2013; Ortíz-Rodríguez et al., 2017; Zanandrea et al., 2020; Zhao et al., 2020), including studies in different areas of China (Zhou et al., 2019; Liu et al., 2020; Zhao et al., 2020). Several modifications on the IC have been made afterwards (Heckmann et al., 2018). Chartin et al. (2017) combined a rainfall erosivity factor with the C factor in the IC to address connectivity better under different rainfall impacts; Gay et al. (2015) integrated a drainage network in the IC to assess connectivity in lowland areas; and López-Vicente and Ben-Salem (2019) introduced the soil permeability and roughness of the terrain factors to refine the local computation of connectivity.

Connectivity in river systems has been investigated generally at spatial scales of 10^{-6}-10^{3} km^2 (Wohl, 2017). Not many studies have investigated connectivity on large basin scale due to the spatial heterogeneity of such large areas and the presence of dams. However, several attempts have been made to aggregate pixel-based IC maps to (sub-) catchment scale (Vigiak et al., 2012; Gay et al. 2015; de Walque et al., 2017; Ortíz-Rodríguez et al., 2017).

The Wei River, with a length of 818 km, is the largest branch of the Yellow River in the Chinese Loess Plateau. During the last three decades, a large number of soil and water conservation measures have been taken by the Chinese government, such as constructing check-dams and terraces and launching the 'Grain-for-Green' project (Wang et al., 2015) in which approximately 12,000 km^2 farmland on steep slopes (≥25°) has been transformed into forest or grassland (Xu and Cao, 2002). It is important to evaluate the impact of these measures and figure out the internal mechanism of sediment reduction for improving the future sustainable land-use strategies (Wei et al., 2020; Wang et al., 2021). In addition, intra-annual (e.g. monthly) variation in vegetation cover and rainfall patterns on the Loess Plateau affects hydrology and potential sediment dynamics, and thus, spatio-temporal patterns of sediment connectivity. Upscaling connectivity studies to larger areas will contribute to a fast method of targeting the sediment hotspots and the areas sensitive to landform change on continental scale (James et al., 2019).

To address the challenge of assessing sediment dynamics in a large river basin with marked heterogeneities, this study evaluated the effects of intra-annual variation on the sediment connectivity. The two research objectives were: (1) to examine the possibility of using the aggregated index of sediment connectivity (AIC) to map and characterize functional and structural sediment connectivity at the large regional scale; and (2) to analyze how the AIC factors determine the monthly sediment connectivity dynamics.

2. Materials and methods

2.1. Study area

The Wei river is the largest tributary of the Yellow River in northwest China (Fig. 1). It originates from Niaoshu Mountain in Gansu Province, crosses Ningxia Province and flows into the Yellow River in Tongguan. The Wei River is 818 km long and has a drainage area of 134,800 km^2. The northern part of the Wei River Basin is the gully area of the Loess Plateau, the southwestern part is the Guanzhong Plain at the foot of the Qinling Mountain. The altitude decreases from northwest to southeast. The average slope in the basin is 13.5°, and ranges from 0°-76.7° with the steepest slopes in the mountain area in the south of the basin and in between the Jing sub-basin and Wei sub-basin (Fig. 1b). The climate zone transits from dry in the northwest to humid in the southeast. The Wei River Basin is located in the continental monsoon climate zone, the winter is cold and dry while the summer is hot and rainy, the annual average precipitation is approximately 559 mm, the potential evapotranspiration is 800–1000 mm, and the annual average natural runoff is 10.4 billion m^3.

Land use and cover in the Wei River Basin consists of cropland, shrubland, herbaceous area, bare land, forest and build-up area (Fig. 1c). The Wei River Basin can be subdivided into three sub-basins —Wei sub-basin (in the south of the basin, 46.1 % of the whole area), Jing sub-basin (in the middle of the basin, 33.85 % of the whole area) and Beiluo sub-basin (in the east of the basin, 20.1 % of the whole area) (Fig. 1a). The Wei sub-basin is the most developed area with many large cities. Vegetation cover in the Jing sub-basin is relatively sparse, natural vegetation was largely degraded due to frequent human activity, degraded grassland and cropland cover 44.5 % and 46.6 % of the catchment, respectively (Xu et al., 2015). In Beiluo sub-basin, vegetation cover improved greatly due to the 'Grain-for-Green' project since 1999, for instance, in Wuqi County in the upper reaches of the Beiluo sub-basin, the percentage of area with vegetation cover greater than 30 % has increased from less than 1 % to 92 % in 2009 (Chen et al., 2016). In addition, numerous soil and water conservation measures have been implemented in the whole catchment since the 1970 s.

2.2. Index of sediment connectivity

The Index of runoff and sediment Connectivity (IC) developed by Borselli et al. (2008) represents the potential connectivity between the different parts of a watershed and a defined target (e.g. outlet, gully, creek, ephemeral stream, river, lake, dam), considering the topographic

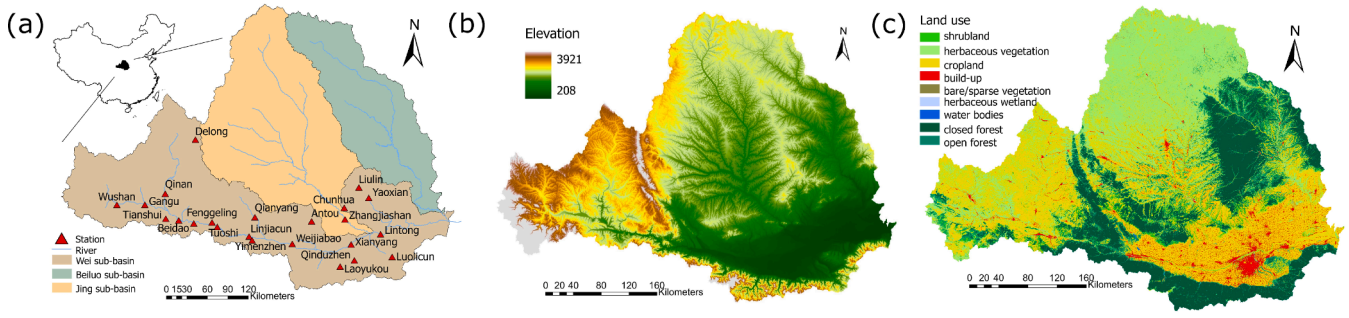

Fig. 1. Wei River Basin study area with (a) location of the sub-catchments, (b) elevation and (c) land use.

and land use conditions of the drainage area, flow path characteristics and flow accumulation along the route. The IC approach is defined in the range of [-∞, +∞] and connectivity increases when the index tends to grow towards +∞. The IC values are dimensionless and strongly depend on the computation target and pixel size, and at each pixel, different values can be obtained due to the index setup (López-Vicente et al., 2021a; López-Vicente et al., 2021b). The IC calculation includes two components: the downslope component (D_{dn}) and the upslope component (D_{up}). D_{dn} represents the probability of sediment to arrive at a sink through the flow path, considering flow length, local conditions and slope gradient. D_{up} is the potential of downward movement of the upslope flow and sediment, depending on local conditions, slope and size of the drainage area. IC is defined as the logarithm of the relationship of D_{dn} and D_{up} (eq. (1)):

$$IC_k = \log_{10}\left(\frac{D_{UP,K}}{D_{dn,k}}\right) = \log_{10}\left(\frac{\overline{W_k} \bullet \overline{S_k}\sqrt{A_k}}{\sum_{i=K,n_k}\frac{d_i}{W_i \bullet S_i}}\right) \quad (1)$$

where $\overline{W}$ is the average weighting factor of sediment transport impedance of the upslope drainage area (dimensionless), $\overline{S}$ is the average slope gradient of the upslope drainage area (m/m), A is the upslope drainage area (m2), d_i is the length of the ith cell along the downslope path (m), W_i is the weight of the ith cell (dimensionless), and S_i is the slope gradient of the ith cell (m/m).In this study we used the Aggregated Index of sediment Connectivity (AIC) introduced by López-Vicente and Ben-Salem (2019) to assess structural and functional connectivity at the catchment scale, taking into account the spatial heterogeneity of rainfall, land use, topography and soil physical properties:

$$AIC_k = \log_{10}\left(\frac{D_{UP,K}}{D_{dn,k}}\right) = \log_{10}\left(\frac{\overline{R_t} \bullet \overline{RT} \bullet \overline{C_t} \bullet \overline{K_P} \bullet \overline{S} \bullet \sqrt{A_K}}{\sum_{k=i}^{n}\frac{d_i}{AWC_i}}\right) \quad (2)$$

$$AWC_i = R_{ti} \bullet RT_i \bullet C_{ti} \bullet K_{pi} \bullet S_i \quad (3)$$

where AWC is the aggregated weighting factor, R_t is the rainfall erosivity factor of the period t, RT is the roughness of the terrain factor, C_t is the vegetation and crop management factor of the period t, K_p is the soil permeability factor, and S is the slope gradient. All the factors were normalized into values between 0.001 and 1. Besides, values of RT and Kp were inversed because higher surface roughness and soil permeability induce lower connectivity (more details about input parameters in (López-Vicente et al., 2021a; López-Vicente et al., 2021b)).

In this study, rainfall erosivity was computed with the method described in Xie et al. (2016):

$$R_{day} = \alpha {P_d}^{1.7265} (P_d > 10mm) \quad (4)$$

where R_{day} is the daily rainfall erosivity, P_d is the daily rainfall amount (including only > 10 mm rainfall), and α is the seasonal coefficient (0.3101 from May to September, 0.3937 from October to April; Xie et al., 2016). Monthly and annual rainfall erosivity were accumulated from the daily rainfall erosivity.

2.3. Data acquisition and analysis

Due to the availability of detailed land use data for the year 2015, and the aim of the study –to analyze the impact and mechanism of large scale vegetation and rainfall variation on sediment discharge–monthly connectivity was quantified using the AIC for the year 2015. To calculate the S and RT factors of the AIC (Eq. (3)), a 30 × 30 m resolution DEM was obtained from Geospatial Data Cloud (https://www.gscloud.cn/) freely. Local sinks were removed using the fill tool in ArcGIS Pro 2.4.3. The S factor was calculated using the slope gradient tool in ArcGIS Pro and normalized between 0.001 and 1. RT was calculated as the inverse values of the standard deviation of the normalized slope gradient.

Monthly precipitation data from 28 meteorological stations within and around the study area of 2015 were obtained from the National Meteorological Information Centre (NMIC) to calculate the rainfall erosivity factor (eq. (4)). The rainfall map was generated using Spline interpolation, and then, the value range was normalized between 0.001 and 1.

To estimate the C factor, yearly and monthly groundcover maps for the region were used from (Yang et al., 2020) and their method to estimate the monthly C factor was used:

$$SLR_i = e^{-0.0418(TC_i - 5)} \quad (5)$$

$$C_i = SLR_i \times EI_i / EI_t \quad (6)$$

$$C = \sum_{i=1}^{12} C_i \quad (7)$$

where SLR_i is the soil loss ratio in month i, TC_i is the total percentage of ground cover, C_i is the monthly C factor in month i,EI_i and EI_t are the monthly and yearly rainfall erosivity respectively.

Finally, the Kp factor was based on soil available water content (between pF2 and pF4.2; m^3/m^3) data, obtained from HiHydroSoil v1.2 (De Boer, 2016). The soil permeability factor (Kp) map was calculated from the normalized and inverse value of soil available water.

In this study the river stream was used as the computation target. Firstly, 20 location of the beginning of the main rivers and tributaries were identified in Google maps. Then, the average value of the flow accumulation map (calculated with the Deterministic Infinity algorithm in ArcGIS Pro 2.4.3) on these 20 locations of the study area was set as the threshold value of the upslope drainage area. Dams and reservoirs larger than 107 m^3 were also included in the computation target map.

The maps of sediment connectivity were generated by running the algorithm procedure in the updated Borselli's index (Ortíz-Rodríguez et al., 2017) combining the AIC weighting factors. Yearly AIC map and monthly AIC maps were calculated following the same procedure but with yearly C factor and rainfall maps, and monthly C factor and rainfall maps, respectively.

Land cover data of 2015 was obtained from (https://lcviewer.vito.be/), and has been used in analyzing different AIC in different land uses. All input and output maps had a pixel resolution of 30 m.

Sediment yield data of 23 hydrological stations of Wei sub-basin and Jing sub-basin (Fig. 1a) were extracted from the China Water Resources Bulletin (Ministry of Water Resources), the consistency and reliability of the data were checked and firmly controlled by the Ministry of Water Resources before data release. The catchment areas of the 23 watersheds were derived using ArcGIS Pro. The average monthly AIC value for each watershed was extracted using the watersheds' catchment areas. Based on this, the Pearson's correlation coefficient (r) between the average monthly AIC and the monthly sediment yield of each watershed was calculated.

3. Results

3.1. Structural sediment connectivity

The AIC connectivity map for the year 2015 (Fig. 2a) shows that values of AIC range from −8.21 to −0.57 with a mean value of −4.26 (standard deviation 1.00). The 10th and 90th percentile values of connectivity (Fig. 2b) show that low connectivity sites are located in the Beiluo sub-basin, with an average AIC value of −4.414 (Table 1). Also in the Guanzhong Plain in the Wei sub-basin and in the central hillslope area of the Jing sub-basin, low connectivity values can be found, indicated by the green color (Fig. 2b). High connectivity areas mainly occur in the Jing sub-basin (with average AIC value of −4.127, Table 1) and in

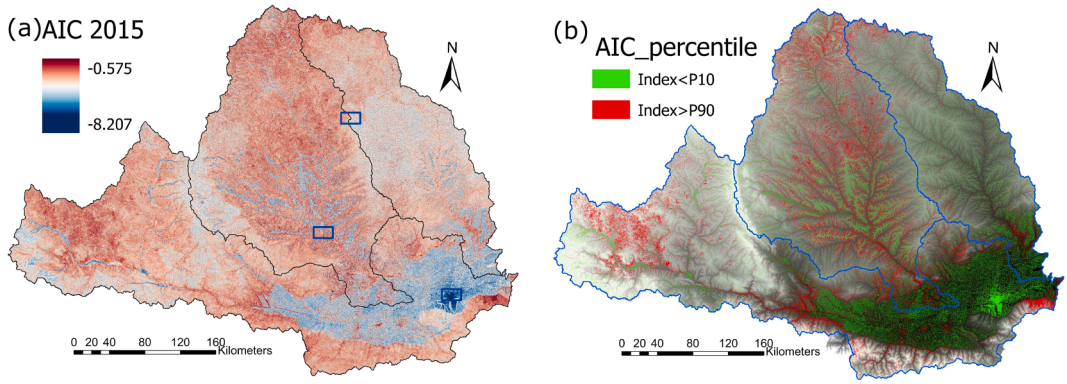

Fig. 2. (a) AIC map and (b) 10th and 90th percentile of AIC for the Wei River Basin in 2015. Blue frames correspond to the zoomed-in areas presented in Fig. 3. (For interpretation of the references to color in this figure legend, the reader is referred to the web version of this article.)

Table 1
Statistics of AIC values in the three main sub-basins of the Wei River Basin.

Sub-catchment:	Mean	Max	Min	STD
Wei sub-basin	−4.309	0.879	−10.319	1.032
Beiluo sub-basin	−4.414	0.248	−9.229	0.919
Jing sub-basin	−4.127	0.809	−9.181	1.011

the east of the Wei sub-basin.

To be able to better visualize the pattern of AIC within the Wei River basin, Fig. 3 shows a zoomed-in map of three locations (see Fig. 2a) of interest and broad occurrence in the Wei River. As would be expected, the forest in the Beiluo sub-basin (right side of the area) has lower sediment connectivity than the crop land (left side of the area) in the Jing sub-basin (Fig. 3a), due to a general higher vegetation cover. However, Fig. 3b zooms in to an area with croplands on the tableland (i.e. higher local plateaus) and shrubland and forest on the hillslopes in Jing sub-basin. Although generally, forest and shrubland would be expected to have lower connectivity due to their higher vegetation coverage compared to cropland (depending on the month, though), Fig. 3b shows that croplands on the tableland have lower sediment connectivity than shrubland and forest on the hillslope. This can be explained by the forested areas locate closer to the target (the river network) and steeper slope. Fig. 3c indicates that the build-up area mostly has a higher connectivity than the cropland area in the plain in the Wei sub-basin, due to a higher C factor in the build-up areas. Here, the relatively low connectivity in the cropland is also affected by the low local slope (flat floodplain area).

We also analyzed the effect of the individual AIC factors (Fig. 4) on the AIC results. The minimum, mean and maximum annual rainfall erosivity was 774.3, 901.1 and 1021.8 MJ mm/ha h yr. The highest rainfall erosivity values appear in the south of the basin (Fig. 4a), while the highest value of AIC is located in the middle and west part of the basin (Fig. 2a), thus the influence of the R factor on the spatial distribution of AIC is relatively low. The roughness of the terrain factor (RT; Fig. 4b) has a mean value of 0.941 (standard deviation 0.043), with the highest and lowest values appearing in the built-up areas and close forest, respectively. The lowest values of slope steepness and higher values of RT are found in the plain area in the Wei sub-basin, while the highest values of the slope factor and lowest values of RT are found in the Qinling Mountain range in the south. The soil permeability factor (Kp) had a mean value of 0.312 (standard deviation 0.031), with lowest values in the mountain ranges where shallower soils occur (Fig. 4d). Fig. 5 shows the distribution of RT, Kp and S factors, as well as the mean AIC for the main land uses. Both RT and Kp do not show large differences between land use, while the slope factor is lowest for the built-up area, that occurs mainly in the relatively flat plain area in the Wei sub-basin and highest for the closed forest. Fig. 4e shows that the C factor is low in the Beiluo sub-basin and the mountain range area in the basin, and is high in the North of the basin. AIC values are clearly lowest for the built-up areas.

3.2. Functional sediment connectivity

The maps of functional sediment connectivity were generated for the 12 months of year 2015. Fig. 6 shows the highest (P90) and lowest (P10) percentiles for months January and April; see supplementary material for maps of all months. Despite the good agreement between the maps of Fig. 6 and the map of percentiles of structural connectivity (Fig. 2b), the maps of the percentiles of functional connectivity illustrate how the spatial location of the areas with the highest and lowest values of connectivity is not fixed, but may evolve over the year according to the

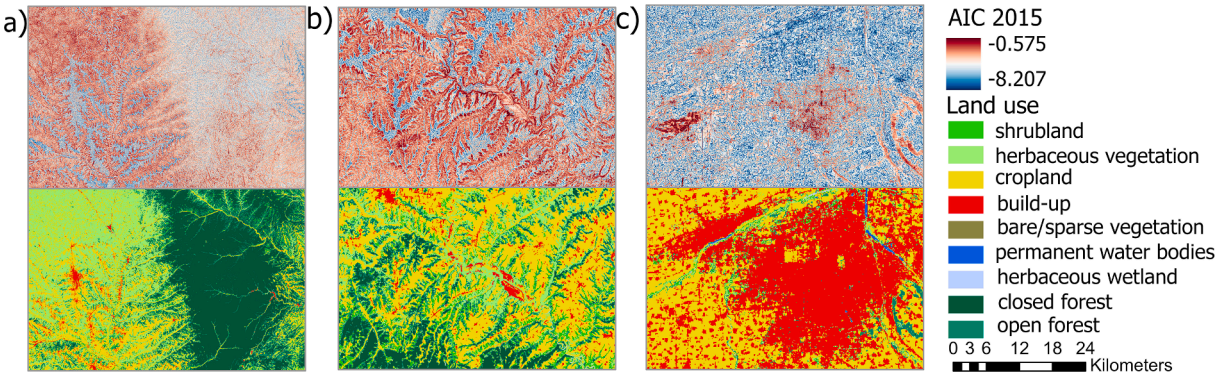

Fig. 3. Detailed map of AIC and land use for three typical areas in the Wei River Basin: (a) forest and cropland in Beiluo and Jing sub-basin, respectively (b) cropland on the tableland and forest/shrubs in the valleys (c) city and surrounding cropland.

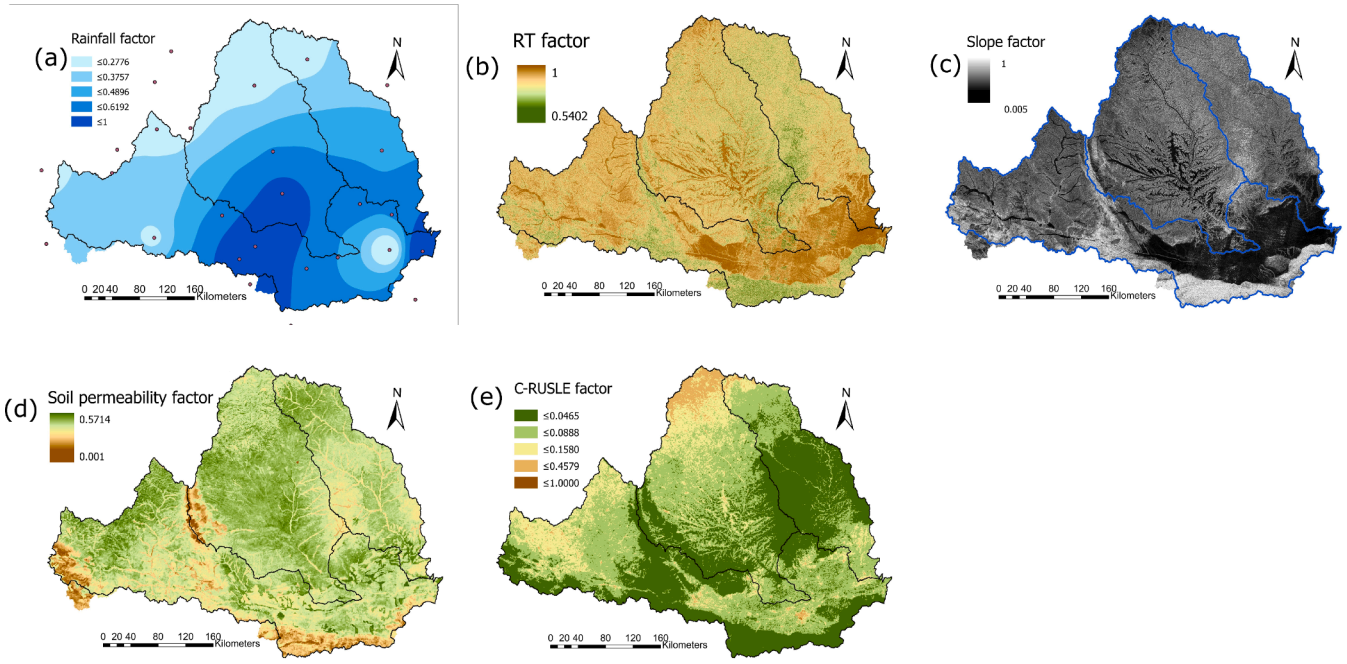

Fig. 4. Maps of the (a) Rainfall factor, (b) roughness of the terrain (RT) factor, (c) slope factor, (d) soil permeability (Kp) factor and (e) C-RUSLE factor.

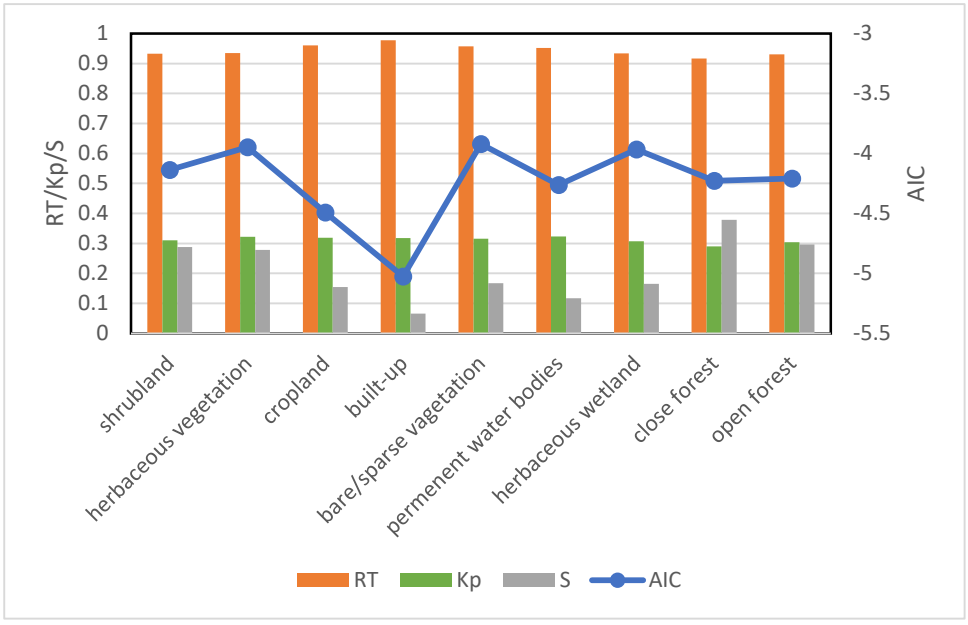

Fig 5. Mean RT (orange), Kp (green) and slope (grey) factor values and AIC (blue line) per land use type. (For interpretation of the references to color in this figure legend, the reader is referred to the web version of this article.)

changes in the spatial and temporal distribution of the values of the R and C factors that are the two inputs with temporal changes. The mean value at basin scale ranged between −8.324 and −6.001. A clear trend can be seen in the mean monthly AIC values for the entire catchment (Fig. 7a) with the lowest AIC values in December, January and February and the highest values in April. In January the high connectivity sites are mainly located in the south (the Qinling mountains) and the north and west part of the basin (Fig. 6a), while in April the highest connectivity sites are located mainly in the Jing sub-basin (Fig. 6b).

The mean values of the C-RUSLE maps (see all monthly maps in supplementary material) at monthly and basin scale ranged from 0.0556 to 0.103 (Fig. 7a). The C-RUSLE factor is relatively high from December to May and relatively low from June to November and is relatively high in the bare land (0.218) and low in the closed forest, open forest and shrubs (Fig. 7b). The highest monthly rainfall was assessed in August, and the lowest from December to February (Fig. 7a). The rainfall factor is low in bare land and no significant difference appears between the other land uses. The standard deviation of the C factor over the 12 months is lower in the Beiluo sub-basin and the mountain range area in between Jing sub-basin and Wei sub-basin (Fig. 8a). Fig. 8a also

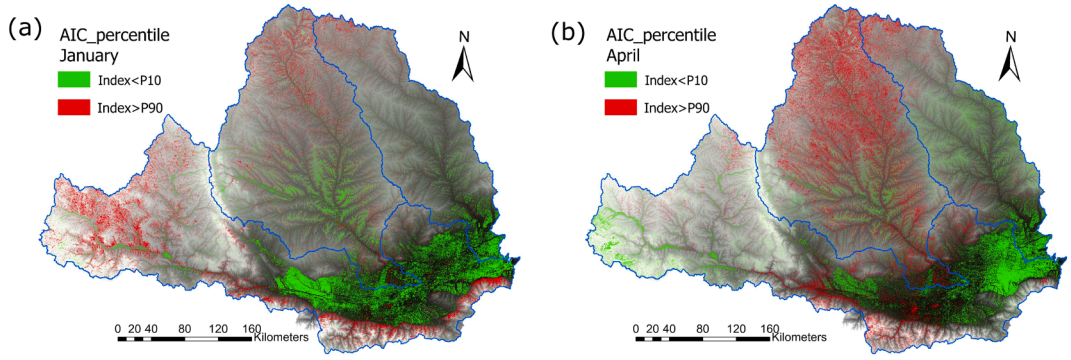

Fig. 6. AIC maps with highest (P90) and lowest (P10) 10% percentiles of AIC values for (a) January 2015 and (b) April 2015.

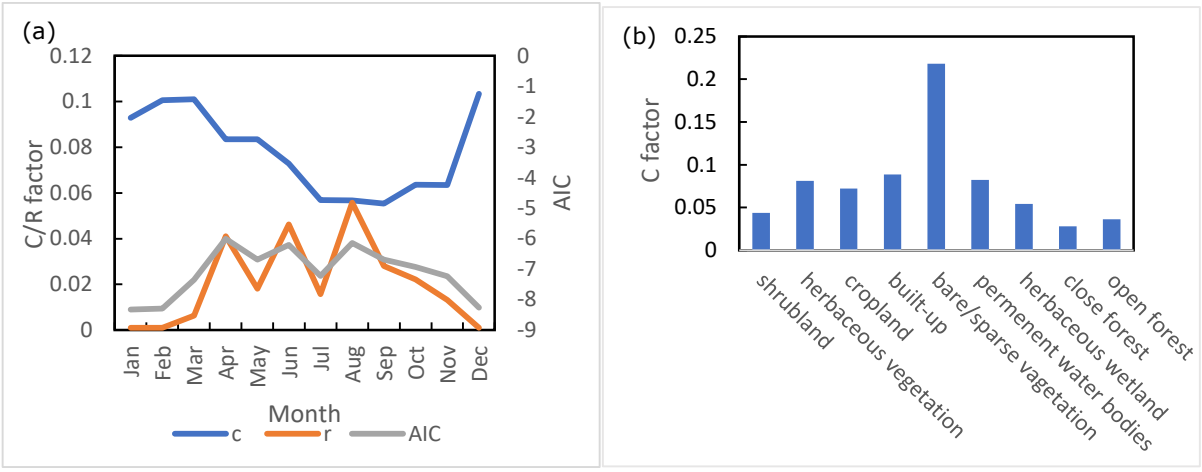

Fig. 7. (a) Mean values of the C-RUSLE factor (C; blue line), Rainfall factor (R; orange line) and AIC values (grey line) per month for the year 2015; and (b) Mean C-factor per land use type. (For interpretation of the references to color in this figure legend, the reader is referred to the web version of this article.)

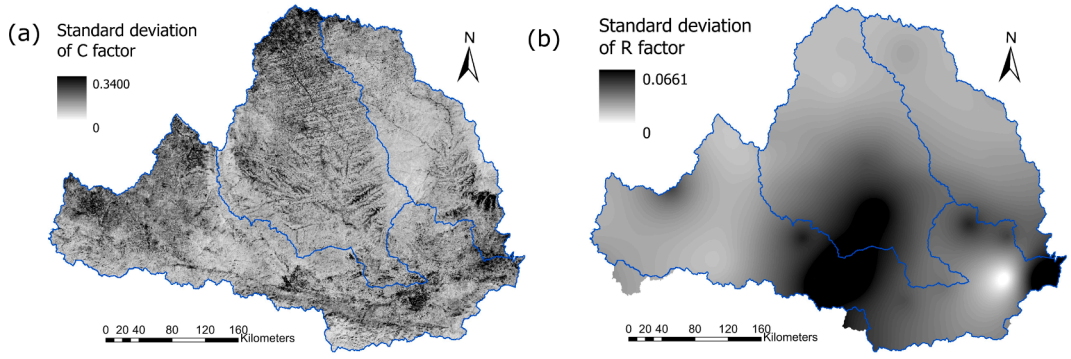

Fig. 8. Standard deviation over the 12 months of 2015 for (a) C-RUSLE factor and (b) R factor.

indicates that changes in the C factor are more intense in the cropland area. Changes in the R factor are more intense in the south of Jing sub-basin and middle part of Wei sub-basin (Fig. 8b).

A linear and negative correlation was found between the average monthly AIC and the C-RUSLE factor (r = -0.61; Fig. 9), while a stronger positive linear correlation was found between the average monthly AIC and mean rainfall erosivity (r = 0.92; Fig. 9).

Fig. 10 shows the temporal trend of the AIC values per land use. The AIC is relatively higher in the herbaceous vegetation (including herbaceous wetland), the shrubland and the forest, while relatively lower in the build-up area, the cropland and the permanent water bodies. The temporal trend does not vary much between land uses, which indicates that the rainfall factor has a stronger effect on the AIC temporal variation than the C-RUSLE factor.

3.3. Validation

The correlation coefficient of mean AIC and sediment yield over 12 months in 2015 of 23 stations (Fig. 1a) in the Wei River Basin were tested: 4 stations showed strong positive correlation, 11 stations showed moderate positive correlation (Table 2.).

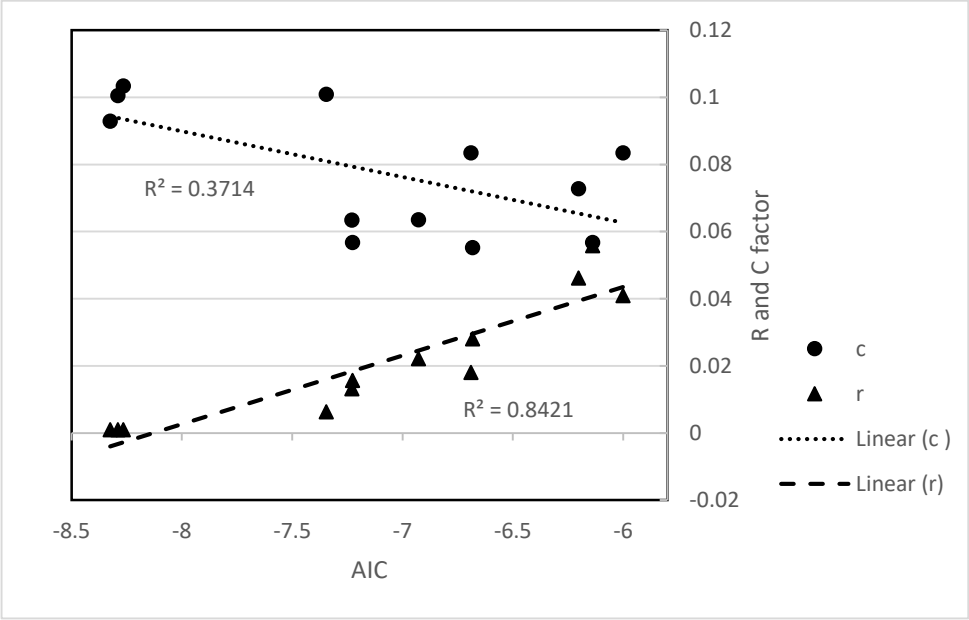

Fig. 9. Relationship between aic and c factor and r factor.

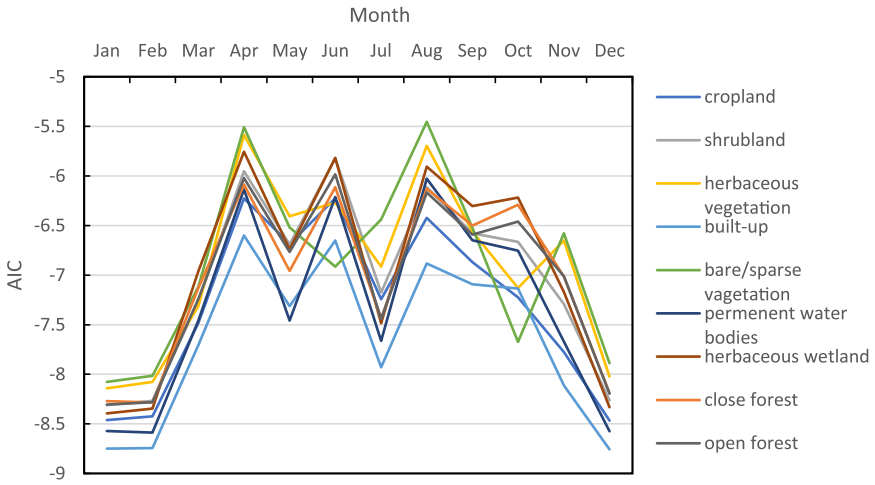

Fig. 10. Monthly AIC value in different land use for the Wei River Basin for the year 2015.

Table 2
Correlation coefficient (r) of monthly mean AIC and sediment yield of 23 stations.

Station	Liulin	Luolicun	Yaoxian	Xianyang	Tuoshi	Qinan	Lintong
r	0.29	0.66**	0.76**	0.66*	0.74**	0.64*	0.48
Huaxian	Fenggeling	Delong	Beidao	Antou	Yimenzhen	Chunhua	Gangu
0.50*	0.78**	0.28	0.67*	0.47	0.55*	0.66*	0.64*
Laoyukou	Linjiacun	Qianyang	Qinduzhen	Tianshui	Weijiabao	Wushan	Zhangjiashan
0.48	0.54*	0.56*	0.39	0.39	0.71*	0.51*	0.46

*$p < 0.1$, **$p < 0.01$.

4. Discussion

The maps of yearly structural connectivity and 10th and 90th percentiles (Fig. 2) show considerable spatial variation within the three catchments in the study area, reflecting the difference of ecological construction and management in these three catchments. The Jing sub-basin has the highest sediment connectivity within the three catchments while Beiluo sub-basin has the lowest. This concurs with the observations and estimations of sediment discharge in these areas. Despite the implementation of various soil and water conservation works in the Jing sub-basin since the 1950 s, the Jing River is still a major sediment source of the Yellow River (Zhang et al., 2020), with an annual sediment transport modulus of Jing sub-basin of 4,776 t/km^2 (Huang et al., 2021). On the other hand, the Grain for Green project has greatly improved the

vegetation cover in the Beiluo sub-basin (Chen et al., 2016), and the average soil erosion modulus of Beiluo sub-basin in 2009 ~ 2018 has been calculated at 358.33 t/(km^2•a) (Hao et al., 2020). Liu et al. (2021) performed scenario simulations and found that vegetation restoration has the potential to reduce sediment connectivity between 20 % and 45 % while conservation constructions such as terraces and check-dams have a potential of 10 %. Coulthard and Van De Wiel (2017) and Llena et al. (2019) reported that afforestation decreases sediment connectivity by increasing surface resistance and roughness. Indeed we found that the Beiluo sub-basin had lower sediment connectivity than the Jing sub-basin due to better ecological conditions.

Our results also agree with a recent study in a small sub-catchment in the Loess Plateau where the highest connectivity area was found along the gullies, and low values in the construction land and vegetation in low slope gradient landscapes (Liu et al., 2022). However in our study, higher sediment connectivity was found in forest areas than in cropland in some instances (Fig. 3ab; Fig. 10). As can be seen in Fig. 1b, cropland is mostly located in the Wei sub-basin on the plain and on gently sloping tableland and in Jing sub-basin on the local plateaus of the tableland, while the forest is located in the steep mountain areas (Fig. 3a). Many studies have shown that forest has lower soil erosion modulus compared to crop land due to higher canopy cover (El Kateb et al., 2013; Liu et al., 2014; Yan et al., 2018), however, the location within the (local) landscape of a certain vegetation type, co-determines the sediment connectivity. This is an important finding of the study: while forest would generally have lower connectivity due to their higher cover, if they are located in steep slopes and gullies, they will still have higher connectivity than cropland (lower cover) on local plateaus (flatter surface) (Wu et al., 2021). This phenomenon can be explained by that sediment connectivity is the potential of sediment delivery between catchment compartments; in the Wei river basin transport is the dominant effect over detachment on sediment connectivity, thus the effect of slope gradient on sediment transport is greater than the effect of landcover on sediment detachment.

As Hooke and Souza (2021) mentioned, validation of the results of sediment connectivity indices is still one of the major challenges in assessing and quantifying connectivity. Some studies have compared or validated connectivity in small catchments (less than 260 km^2) using field mapping (Messenzehl et al., 2014; Nicoll and Brierley, 2017), but in a large river basin like the Wei river basin this task is challenging, since the connection of every part of the system need to be assessed, thus in this study we assessed the correlation of sediment yield and functional connectivity as an attempt to validate the results, 15 stations showed significant positive correlation among 23 watersheds, 8 stations showed insignificant correlation due to the sediment yield of these stations peak in July and August within the year while AIC peak in Aril, June and August (Fig. 7a). A possible explanation is that in the Chinese Loess Plateau summer is the wet season, rainfall is intense and concentrate in short time, thus the sediment yield is high in July and August. While in April the amount of rainfall is large but spread over the month, therefore the potential of sediment flux oncoming from the catchment reaching the stream and reservoir is high. The rainfall erosivity factor hasn't present the difference which need to be improved in the future study. Moreover, this study used river stream and reservoir as the target of sediment connectivity, the process of sediment travel from river stream to the catchment outlet can be affected by many factors, such as travel time, travel distance and sediment residence time within the catchment, thus the sediment yield result of the 8 stations may have low correlation with the AIC result.

The AIC as a numerical approach can be helpful for monitoring potential sediment transport in ungauged areas, especially in developing countries like China where spatial data is often scarce. It requires limited computing requirements and time (López-Vicente et al., 2021a; López-Vicente et al., 2021b), while still taking topography, vegetation, soil and rainfall conditions into consideration. When comparing with the widely used Universal Soil Loss Equation (USLE) (Borrelli et al., 2017), AIC has an impressive advantage: the USLE targets at on site soil erosion, originally developed for plot scale of 22.1 m length (Alewell et al., 2019), however, the AIC calculates long slope dynamics from flow accumulation and taking river channels into account. Moreover, compared to the usage of SDR (sediment delivery ratio), AIC provides insight of the processes that take place between the sediment sources and sinks as well as their connection to the watershed outlet (Hoffmann, 2015). Najafi (2021) reviewed sediment connectivity studies from 1997 to 2019, showing that most studies were carried out in small watershed scale. Our study applied AIC in a large basin of 134,800 km^2 with the AIC results from 15 of 23 stations showing strong or moderate positive relation with measured sediment yield. Thus, the AIC calculation can be a useful indicator for local managers to obtain information of large scale sediment delivery and to identify sediment source and sink areas.

Najafi (2021) also pointed out that most current sediment connectivity studies are based on structural connectivity due to the usefulness of site prioritization in sediment management and the limitation on methodology. However, functional connectivity did not receive enough attention (Najafi et al. 2021). Functional connectivity is a process-based concept related to the interaction of soil erosion and sediment yield processes under hydrological influences (López-Vicente et al. 2020). In this study, five factors have been used to calculate the sediment connectivity index, in which the rainfall factor showed the strongest correlation with AIC, indicating that AIC is able to illustrate the hydrological and erosional responses of the system processes at different spatio-temporal scales (Thompson et al., 2013; Williams et al., 2016; Turnbull and Wainwright 2019). Functional connectivity can also give insight into the functioning of vegetation cover during different seasons: the monthly AIC maps (Supplement 1) provide dynamic information on high sediment connectivity areas consistent with vegetation patterns. In this study, intra-annual connectivity dynamics were evaluated and unraveled for the Wei River basin. While 2015 was a dry year in terms of annual rainfall and monthly changes in vegetation cover are important for agricultural land uses, longer-term (i.e. decadal) changes in land cover and trends in rainfall affect connectivity dynamics on longer timescales. Also, the effects of gradual (i.e. covering multiple years) implementation of soil and water conservation measures in various subcatchments can only be evaluated on longer timescales. Therefore, further research will include testing the functional sediment connectivity of the land-use changes on decadal timescales, including assessing changing sediment discharge data in the Wei River Basin.

Moreover, there are more factors that may lead to changes in sediment connectivity that need to be included in the future research, such as implementation of soil and water conservation measures (Sandercock and Hooke, 2011). In this study only large and medium-sized reservoirs listed in the Global Reservoir and Dam dataset were accounted for as sink (dis-connectivity), yet since 2002, about 113,500 small scale check-dams have been built in the Loess Plateau which intercepted approximately 700 million m^3 of sediment (Xiang-zhou et al., 2004). As they play a critical role in (local) sediment yield reduction (Zhao et al., 2020; Feng et al., 2021), check-dams should be targeted as sinks when the location data is available and the pixel size of the DEM allows their representation as an input of AIC (González-Romero et al., 2021). Recent studies suggest that remote sensing can be introduced to assess the site of the check-dams (Rajendran et al., 2020; Guan et al., 2021). When calculating the index of connectivity (IC), which AIC was based on, originally a weighting factor was used to represent the ground cover and surface roughness that would obstruct water and sediment fluxes according to the characteristics of the study area. Borselli et al. (2008) proposed to use C-RUSLE factor as the weighting factor for regions where vegetation cover has a big impact on sediment transport. (Morresi et al., 2019; Martini et al., 2020) proposed weighting factors of the Manning's n for the overland flow combined with the Integrated Forest Z-score or NDVI. Thus, we suggest that a new weight can be assigned to the C factor in AIC to adjust the impact of overland flow velocity in future studies. Plot study or sediment discharge data can be used to

calibrate this weight considering the situation of the study area.

5. Conclusions

This study proved the ability of the AIC to map and calculate structural and functional sediment connectivity at a large regional scale like the Wei River Basin in the Loess Plateau, China. The connectivity maps, at monthly and yearly scale, have identified the potential sediment hotspots and the impact of spatially varying cover due to ecological restoration on the sediment regime.

The three sub-basins showed significant differences due to the different ecological restoration conditions. Regarding structural connectivity, high connectivity areas were found in the west part of the Wei sub-basin and the Jing sub-basin, and low connectivity areas were located in the east part of the Wei sub-basin and the Beiluo sub-basin. Within the different land uses, bare land had the highest connectivity (-3.92), while build-up area had the lowest (-5.03), cropland on the tableland had lower connectivity than shrubland and forest on the hill slope, indicating that location (transport: distance to the stream) and topographic conditions (velocity: slope gradient) has greater impact than land cover (soil particle detachment and rainfall interception) on sediment connectivity. Functional connectivity showed that highest and lowest connectivity occurred in April (-6.00) and January (-8.42), respectively, due to the wet season starting from April and the growing season from April to September. Sediment yield from 15 of 23 hydrological stations in the study area showed strong or moderate positive correlation with the AIC results. The rainfall factor showed the highest correlation with AIC, and thus, functional connectivity represented sediment dynamics better than structural connectivity.

With consideration of both topographic features (i.e. structural connectivity) and rainfall and land cover conditions (i.e. functional connectivity), AIC shows great potential for large scale soil erosion hotspot research and investigation of spatial–temporal land-use and climate change effects on sediment yield dynamics.

CRediT authorship contribution statement

Zhenni Wu: Conceptualization, Validation, Formal analysis, Writing – original draft. **Jantiene E.M. Baartman:** Conceptualization, Supervision, Writing – review & editing. **João Pedro Nunes:** Conceptualization, Supervision, Writing – review & editing. **Manuel López-Vicente:** Methodology, Software.

Declaration of Competing Interest

The authors declare that they have no known competing financial interests or personal relationships that could have appeared to influence the work reported in this paper.

Data availability

Data will be made available on request.

Acknowledgements

The China Scholarship Council funded this work through the grant attributed to Z Wu (CSC: 201906300050). The authors would like to acknowledge Prof. Xihua Yang for providing his research findings and data for the C-RUSLE factor preparation in this study.

Appendix A. Supplementary data

Supplementary data to this article can be found online at https://doi.org/10.1016/j.ecolind.2022.109775.

References

Alewell, C., Borrelli, P., Meusburger, K., Panagos, P., 2019. Using the USLE: Chances, challenges and limitations of soil erosion modelling. Int. Soil Water Conservat. Res. 7 (3), 203–225.
Borrelli, P., Robinson, D.A., Fleischer, L.R., Lugato, E., Ballabio, C., Alewell, C., Meusburger, K., Modugno, S., Schutt, B., Ferro, V., Bagarello, V., Oost, K.V., Montanarella, L., Panagos, P., 2017. An assessment of the global impact of 21st century land use change on soil erosion. Nat. Commun. 8 (1), 2013.
Borselli, L., Cassi, P., Torri, D., 2008. Prolegomena to sediment and flow connectivity in the landscape: A GIS and field numerical assessment. Catena 75 (3), 268–277.
Bracken, L.J., Turnbull, L., Wainwright, J., Bogaart, P., 2015. Sediment connectivity: a framework for understanding sediment transfer at multiple scales. Earth Surf. Proc. Land. 40 (2), 177–188.
Chartin, C., O. Evrard, J. P. Laceby, Y. Onda, C. Ottlé, I. Lefèvre and O. Cerdan (2017). "The impact of typhoons on sediment connectivity: lessons learnt from contaminated coastal catchments of the Fukushima Prefecture (Japan)." Earth Surf. Process. Landfor. 42(2): 306–317.
Chen, N., Ma, T., Zhang, X., 2016. Responses of soil erosion processes to land cover changes in the Loess Plateau of China: A case study on the Beiluo River basin. Catena 136, 118–127.
Cossart, É., Fressard, M., 2017. Assessment of structural sediment connectivity within catchments: insights from graph theory. Earth Surf. Dyn. 5 (2), 253–268.
Coulthard, T.J., Van De Wiel, M.J., 2017. Modelling long term basin scale sediment connectivity, driven by spatial land use changes. Geomorphology 277, 265–281.
De Boer, F.(2016). "HiHydroSoil: A High Resolution Soil Map of Hydraulic Properties Version 1.2." FutureWater report 134. Wageningen.
de Walque, B., Degré, A., Maugnard, A., Bielders, C.L., 2017. Artificial surfaces characteristics and sediment connectivity explain muddy flood hazard in Wallonia. Catena 158, 89–101.
El Kateb, H., Zhang, H., Zhang, P., Mosandl, R., 2013. Soil erosion and surface runoff on different vegetation covers and slope gradients: A field experiment in Southern Shaanxi Province, China. Catena 105, 1–10.
Feng, Z., Li, Z., Shi, P., Li, P., Wang, T., Duan, J., 2021. Impact of sedimentation by check dam on the hydrodynamics in the channel on the Loess Plateau of China. Nat. Hazards 107 (1), 953–969.
Fu, B., Liu, Y., Lü, Y., He, C., Zeng, Y., Wu, B., 2011. Assessing the soil erosion control service of ecosystems change in the Loess Plateau of China. Ecol. Complex. 8 (4), 284–293.
Gay, A., Cerdan, O., Mardhel, V., Desmet, M., 2015. Application of an index of sediment connectivity in a lowland area. J. Soil. Sediment. 16 (1), 280–293.
González-Romero, J., López-Vicente, M., Gómez-Sánchez, E., Peña-Molina, E., Galletero, P., Plaza-Alvarez, P., Moya, D., De las Heras, J., Lucas-Borja, M.E., 2021. Post-fire management effects on sediment (dis)connectivity in Mediterranean forest ecosystems: Channel and catchment response. Earth Surf. Proc. Land. 46 (13), 2710–2727.
Gu, C., Mu, X., Gao, P., Zhao, G., Sun, W., Tan, X., 2019. Distinguishing the effects of vegetation restoration on runoff and sediment generation on simulated rainfall on the hillslopes of the loess plateau of China. Plant Soil 447 (1–2), 393–412.
Guan, T., Xu, Q., Chen, X., Cai, J., 2021. A novel remote sensing method to determine reservoir characteristic curves using high-resolution data. Hydrol. Res.
Hao, G.R., Li, J.K., Li, S., Li, K.B., Zhang, Z.H., Li, H.E., 2020. Quantitative assessment of non-point source pollution load of PN/PP based on RUSLE model: a case study in Beiluo River Basin in China. Environ. Sci. Pollut. Res. Int. 27 (27), 33975–33989.
Heckmann, T., Cavalli, M., Cerdan, O., Foerster, S., Javaux, M., Lode, E., Smetanová, A., Vericat, D., Brardinoni, F., 2018. Indices of sediment connectivity: opportunities, challenges and limitations. Earth Sci. Rev. 187, 77–108.
Hoffmann, T., 2015. Sediment residence time and connectivity in non-equilibrium and transient geomorphic systems. Earth Sci. Rev. 150, 609–627.
Hooke, J., Souza, J., 2021. Challenges of mapping, modelling and quantifying sediment connectivity. Earth Sci. Rev. 223.
Huang, C., Yang, Q., Huang, W., 2021. Analysis of the Spatial and Temporal Changes of NDVI and Its Driving Factors in the Wei and Jing River Basins. Int. J. Environ. Res. Public Health 18 (22).
Huo, A., Yang, L., Luo, P., Cheng, Y., Peng, J., Nover, D., 2021. Influence of landfill and land use scenario on runoff, evapotranspiration, and sediment yield over the Chinese Loess Plateau. Ecol. Ind. 121.
Issaka, S., Ashraf, M.A., 2017. Impact of soil erosion and degradation on water quality: a review. Geol., Ecol. Landscapes 1 (1), 1–11.
James, L.A., Monohan, C., Ertis, B., 2019. Long-term hydraulic mining sediment budgets: Connectivity as a management tool. Sci. Total Environ. 651 (Pt 2), 2024–2035.
Lisenby, P.E., Fryirs, K.A., Thompson, C.J., 2019. River sensitivity and sediment connectivity as tools for assessing future geomorphic channel behavior. Int. J. River Basin Manage. 18 (3), 279–293.
Liu, Y., Cui, B., Du, J., Wang, Q., Yu, S., Yang, W., 2020. A method for evaluating the longitudinal functional connectivity of a river–lake–marsh system and its application in China. Hydrol. Process. 34 (26), 5278–5297.
Liu, W., Shi, C., Ma, Y., Li, H., Ma, X., 2021. Land use and land cover change-induced changes of sediment connectivity and their effects on sediment yield in a catchment on the Loess Plateau in China. Catena 207.
Liu, W., Shi, C., Ma, Y., Wang, Y., 2022. Evaluating sediment connectivity and its effects on sediment reduction in a catchment on the Loess Plateau, China. Geoderma 408.
Liu, Y.J., Wang, T.W., Cai, C.F., Li, Z.X., Cheng, D.B., 2014. Effects of vegetation on runoff generation, sediment yield and soil shear strength on road-side slopes under a simulation rainfall test in the Three Gorges Reservoir Area, China. Sci. Total Environ. 485–486, 93–102.

Llena, M., Vericat, D., Cavalli, M., Crema, S., Smith, M.W., 2019. The effects of land use and topographic changes on sediment connectivity in mountain catchments. Sci. Total Environ. 660, 899–912.
López-Vicente, M., Ben-Salem, N., 2019. Computing structural and functional flow and sediment connectivity with a new aggregated index: A case study in a large Mediterranean catchment. Sci. Total Environ. 651 (Pt 1), 179–191.
López-Vicente, M., Lana-Renault, N., García-Ruiz, J.M., Navas, A., 2011. Assessing the potential effect of different land cover management practices on sediment yield from an abandoned farmland catchment in the Spanish Pyrenees. J. Soil. Sediment. 11 (8), 1440–1455.
López-Vicente, M., Poesen, J., Navas, A., Gaspar, L., 2013. Predicting runoff and sediment connectivity and soil erosion by water for different land use scenarios in the Spanish Pre-Pyrenees. Catena 102, 62–73.
López-Vicente, M., Nadal-Romero, E., Cammeraat, E.L.H., 2016. Hydrological Connectivity Does Change Over 70 Years of Abandonment and Afforestation in the Spanish Pyrenees. Land Degrad. Dev. 28 (4), 1298–1310.
López-Vicente, M., González-Romero, J., Lucas-Borja, M.E., 2020. Forest fire effects on sediment connectivity in headwater sub-catchments: Evaluation of indices performance. Sci. Total Environ. 732, 139206.
López-Vicente, M., Cerdà, A., Kramer, H., Keesstra, S., 2021a. Post-fire practices benefits on vegetation recovery and soil conservation in a Mediterranean area. Land Use Policy 111, 105776.
López-Vicente, M., Kramer, H., Keesstra, S., 2021b. Effectiveness of soil erosion barriers to reduce sediment connectivity at small basin scale in a fire-affected forest. J. Environ. Manage. 278 (Pt 1), 111510.
Martini, L., Faes, L., Picco, L., Iroume, A., Lingua, E., Garbarino, M., Cavalli, M., 2020. Assessing the effect of fire severity on sediment connectivity in central Chile. Sci. Total Environ. 728, 139006.
Messenzehl, K., Hoffmann, T., Dikau, R., 2014. Sediment connectivity in the high-alpine valley of Val Müschauns, Swiss National Park — linking geomorphic field mapping with geomorphometric modelling. Geomorphology 221, 215–229.
Morresi, D., Vitali, A., Urbinati, C., Garbarino, M., 2019. Forest Spectral Recovery and Regeneration Dynamics in Stand-Replacing Wildfires of Central Apennines Derived from Landsat Time Series. Remote Sens. (Basel) 11 (3).
Najafi, S., D. Dragovich, T. Heckmann and S. H. Sadeghi (2021). "Sediment connectivity concepts and approaches." Catena 196.
NDRC, MWR, MA, SFA National Development and Reform Commission, Ministry of Water Resources, Ministry of Agriculture, State Forestry Administration (2010). People's Republic of China. (in Chinese).
Nicoll, T., Brierley, G., 2017. Within-catchment variability in landscape connectivity measures in the Garang catchment, upper Yellow River. Geomorphology 277, 197–209.
Ortíz-Rodríguez, A.J., Borselli, L., Sarocchi, D., 2017. Flow connectivity in active volcanic areas: Use of index of connectivity in the assessment of lateral flow contribution to main streams. Catena 157, 90–111.
Pimentel, D., 2006. Soil Erosion: A Food and Environmental Threat. Environ. Dev. Sustain. 8 (1), 119–137.
Rajendran, S., Nasir, S., Jabri, K.A., 2020. Mapping and accuracy assessment of siltation of recharge dams using remote sensing technique. Sci. Rep. 10 (1).
Sandercock, P.J., Hooke, J.M., 2011. Vegetation effects on sediment connectivity and processes in an ephemeral channel in SE Spain. J. Arid Environ. 75 (3), 239–254.
Thompson, J., Cassidy, R., Doody, D.G., Flynn, R., 2013. Predicting critical source areas of sediment in headwater catchments. Agr. Ecosyst. Environ. 179, 41–52.
Tong, L.S., Fang, N.F., Xiao, H.B., Shi, Z.H., 2020. Sediment deposition changes the relationship between soil organic and inorganic carbon: Evidence from the Chinese Loess Plateau. Agr. Ecosyst. Environ. 302.
Turnbull, L., Wainwright, J., 2019. From structure to function: Understanding shrub encroachment in drylands using hydrological and sediment connectivity. Ecol. Ind. 98, 608–618.
Turnbull, L., Wainwright, J., Brazier, R.E., 2008. A conceptual framework for understanding semi-arid land degradation: ecohydrological interactions across multiple-space and time scales. Ecohydrology 1 (1), 23–34.
Vigiak, O., Borselli, L., Newham, L.T.H., McInnes, J., Roberts, A.M., 2012. Comparison of conceptual landscape metrics to define hillslope-scale sediment delivery ratio. Geomorphology 138, 74–88.
Wang, S., Fu, B., Piao, S., Lü, Y., Ciais, P., Feng, X., Wang, Y., 2015. Reduced sediment transport in the Yellow River due to anthropogenic changes. Nat. Geosci. 9 (1), 38–41.
Wang, J., Liu, Z., Gao, J., Emanuele, L., Ren, Y., Shao, M., Wei, X., 2021. The Grain for Green project eliminated the effect of soil erosion on organic carbon on China's Loess Plateau between 1980 and 2008. Agr. Ecosyst. Environ. 322, 107636.
Wen, X. and L. Zhen (2020). "Soil erosion control practices in the Chinese Loess Plateau: A systematic review." Environmental Development **34**.
Wei, W., Wang, B., Niu, X., 2020. Soil Erosion Reduction by Grain for Green Project in Desertification Areas of Northern China. Forests 11 (4).
Williams, C.J., Pierson, F.B., Robichaud, P.R., Al-Hamdan, O.Z., Boll, J., Strand, E.K., 2016. Structural and functional connectivity as a driver of hillslope erosion following disturbance. Int. J. Wildland Fire 25 (3).
Wohl, E., 2017. Connectivity in rivers. Progr. Phys. Geograp.: Earth Environ. 41 (3), 345–362.
Wohl, E., Brierley, G., Cadol, D., Coulthard, T.J., Covino, T., Fryirs, K.A., Grant, G., Hilton, R.G., Lane, S.N., Magilligan, F.J., Meitzen, K.M., Passalacqua, P., Poeppl, R. E., Rathburn, S.L., Sklar, L.S., 2019. Connectivity as an emergent property of geomorphic systems. Earth Surf. Proc. Land. 44 (1), 4–26.
Wu, J., Baartman, J.E.M., Nunes, J.P., 2021. Testing the impacts of wildfire on hydrological and sediment response using the OpenLISEM model. Part 2: Analyzing the effects of storm return period and extreme events. Catena 207.
Xiang-zhou, X., Hong-wu, Z., Ouyang, Z., 2004. Development of check-dam systems in gullies on the Loess Plateau, China. Environ. Sci. Policy 7 (2), 79–86.
Xie, Y., Yin, S.-Q., Liu, B.-Y., Nearing, M.A., Zhao, Y., 2016. Models for estimating daily rainfall erosivity in China. J. Hydrol. 535, 547–558.
Xu, J., Cao, Y., 2002. Efficiency and Sustainability of Converting Cropland to Forest and Grassland in The Western Region. Implementing The Natural Forest Protection Program and The Sloping Land Conversion Program: Lessons and Policy Implications CCICED-WCFGTF. China Forestry Publishing House, Beijing. (In Chinese).
Xu, L., Shi, Z., Wang, Y., Zhang, S., Chu, X., Yu, P., Xiong, W., Zuo, H., Wang, Y., 2015. Spatiotemporal variation and driving forces of reference evapotranspiration in Jing River Basin, northwest China. Hydrol. Process. 29 (23), 4846–4862.
Yan, R., Zhang, X., Yan, S., Chen, H., 2018. Estimating soil erosion response to land use/cover change in a catchment of the Loess Plateau, China. Int. Soil Water Conserv. Res. 6 (1), 13–22.
Yang, X., X. Zhang, D. Lv, S. Yin, M. Zhang, Q. Zhu, Q. Yu (2020). "Remote sensing estimation of the soil erosion cover-management factor over China's Loess Plateau." Land Degradation & Development.
Zanandrea, F., Michel, G.P., Kobiyama, M., 2020. Impedance influence on the index of sediment connectivity in a forested mountainous catchment. Geomorphology 351.
Zhang, J., Shang, Y., Liu, J., Fu, J., Wei, S., Tong, L., 2020. Causes of Variations in Sediment Yield in the Jinghe River Basin, China. Sci. Rep. 10 (1), 18054.
Zhao, G., P. Gao, P. Tian, W. Sun, J. Hu, X. Mu (2020). "Assessing sediment connectivity and soil erosion by water in a representative catchment on the Loess Plateau, China." Catena 185.
Zhou, M., Deng, J., Lin, Y., Belete, M., Wang, K., Comber, A., Huang, L., Gan, M., 2019. Identifying the effects of land use change on sediment export: Integrating sediment source and sediment delivery in the Qiantang River Basin, China. Sci. Total Environ. 686, 38–49.